



AIAA 2003-1924

**A Harmonic Balance Approach for
Modeling Nonlinear Aeroelastic Behavior
of Wings in Transonic Viscous Flow**

Jeffrey P. Thomas, Kenneth C. Hall, and Earl H. Dowell
Duke University, Durham, NC 27708-0300

**44th AIAA/ASME/ASCE/AHS/ASC
Structures, Structural Dynamics, and Materials
Conference and Exhibit
April 7-10, 2003/Norfolk, VA**

A Harmonic Balance Approach for Modeling Nonlinear Aeroelastic Behavior of Wings in Transonic Viscous Flow

Jeffrey P. Thomas, * Kenneth C. Hall, † and Earl H. Dowell ‡
Duke University, Durham, NC 27708–0300

Presented is a frequency-domain harmonic-balance (HB) computational fluid dynamic (CFD) approach for modeling flutter onset and limit cycle oscillation (LCO) behavior of viscous transonic aeroelastic wing configurations. The AGARD 445.6 transonic wing configuration is studied and results are compared to a recent inviscid analysis for a supersonic Mach number flow condition.

Nomenclature

A_R	= aspect ratio = wing span squared/wing area
b, c	= wing root semi-chord and chord, respectively
\mathbf{C}_Q	= vector of non-dimensional generalized forces
\mathbf{I}	= identity matrix
\bar{m}	= mass of wing
M_∞	= free-stream Mach number
M	= number of structural modes
\mathcal{M}	= generalized mass matrix
\bar{p}_1	= first harmonic unsteady pressure
\mathbf{Q}	= vector of generalized aerodynamic forces
q_∞	= free-stream dynamic pressure
Re_∞	= free-stream Reynolds number
ρ_∞	= free-stream density
U_∞	= free-stream velocity
\bar{v}	= volume of a truncated cone having stream-wise root chord as lower base diameter, stream-wise tip chord as upper base diameter, and wing half span as height
V	= reduced velocity $V = U_\infty / \sqrt{\mu} \omega_\alpha b$
α_0	= wing steady (or mean) flow angle-of-attack
λ_t	= wing taper ratio $\lambda_t = c_t / c_r$
μ	= mass ratio, $\mu = \bar{m} / \rho_\infty \bar{v}$
ψ_m	= m^{th} structural mode shape
$\omega, \bar{\omega}$	= frequency and reduced frequency $\bar{\omega} = \omega b / U_\infty$
ω_α	= wing first torsional mode natural frequency
$\mathbf{\Omega}$	= matrix with structural frequency ratios squared along main diagonal (e.g. $(\omega_1 / \omega_\alpha)^2, \dots, (\omega_M / \omega_\alpha)^2$)
$\xi_m, \boldsymbol{\xi}$	= m^{th} modal structural coordinate and vector of modal structural coordinates

*Research Assistant Professor, Department of Mechanical Engineering and Materials Science, Member AIAA

†Professor and Department Chairperson, Department of Mechanical Engineering and Materials Science, Associate Fellow AIAA

‡J. A. Jones Professor, Department of Mechanical Engineering and Materials Science, and Dean Emeritus, School of Engineering, Fellow AIAA

Copyright © 2003 by Jeffrey P. Thomas, Kenneth C. Hall, and Earl H. Dowell. Published by the American Institute of Aeronautics and Astronautics, Inc. with permission.

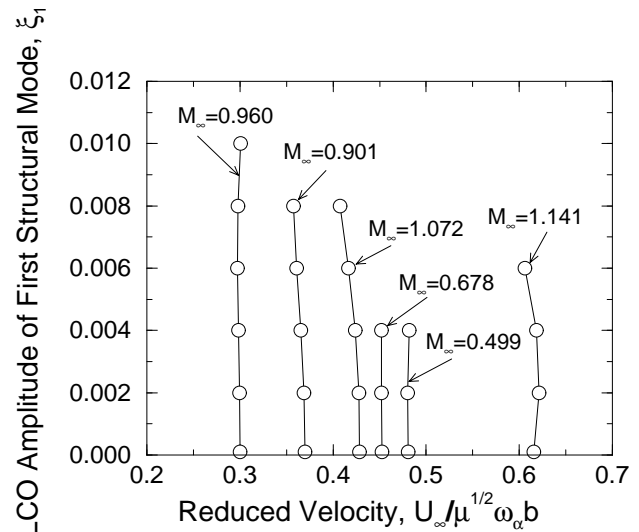


Fig. 1 Computed AGARD 445.6 Wing Configuration LCO Behavior Trends for Inviscid Flow Model. From Ref. [4]

Introduction

Over the course of the last several years, significant progress has been made by our research group towards developing a frequency-domain harmonic balance (HB) approach for modeling nonlinear unsteady aerodynamics and aeroelasticity. The HB method provides an alternative to time-domain approaches, and it can be implemented within the framework of any conventional computational fluid dynamic (CFD) solver method. Details of the method can be found in Hall et. al.¹ and Thomas et. al.² In these references, the use of the technique to model limit cycle oscillation (LCO) behavior of viscous flow compressor and inviscid flow airfoil configurations is demonstrated. Recently Thomas et. al.³ presented viscous flow airfoil LCO results using the methodology for an experimental benchmark transonic aeroelastic configuration of an NLR 7301 airfoil section where it has been demonstrated that accounting for viscous effects significantly

influences the predicted LCO behavior trends. There, viscous effects are shown to produce a more benign LCO trend when compared to an inviscid flow model.

In another paper, Thomas et. al.⁴ also recently demonstrated the HB/LCO solution methodology applied to an inviscid flow model of the well known benchmark AGARD 445.6 transonic wing configuration.^{5,6} For that particular inviscid flow analysis, benign LCO behavior is not observed per se. That is, the amplitude of the aeroelastic motion is predicted to increase rapidly as one considers reduced velocities beyond the flutter onset condition. Figure. 1 shows computed LCO behavior trends for an inviscid flow model of the AGARD 445.6 wing configuration as presented in Ref [4]. Plotted in Fig. 1 is the LCO amplitude of the first structural modal coordinate, ξ_1 , versus the reduced velocity V for six different Mach numbers. The data points for zero LCO amplitude correspond to the flutter onset condition. Note how the LCO curves are nearly vertical. This is indicative of very linear aeroelastic LCO response behavior.

The objective of the current study is to now consider a viscous flow model for the AGARD 445.6 configuration and to assess what effects viscosity may have on LCO. For the two-dimensional results studied in Ref. [3], it has been observed that shock induced boundary layer separation appears to be a primary factor influencing overall LCO. We seek to determine whether a similar effect is also evident, and to what extent, for the AGARD 445.6 configuration, and to determine if the shape of the LCO curve changes for the highest Mach number considered in the inviscid analysis. We aim to determine if a more benign LCO trend will be observed due to nonlinear effects brought about by shock induced boundary layer separation on the wing. That is, as one considers reduced velocities beyond the flutter onset condition, the amplitude of the LCO motion will instead be predicted to grow more gradually with ever increasing reduced velocity. Previous investigations⁷⁻⁹ have observed that accounting for viscous effects plays a significant role in accurately predicting the flutter onset conditions, especially so for the supersonic Mach numbers.

Aeroelastic Model Governing Equations

Following the same development as Ref. [4], the governing aeroelastic system of equations for the AGARD 445.6 wing configuration may be written in the frequency domain as:

$$k_w \mathcal{M} \left(-\bar{\omega}^2 \mu \mathbf{I} + \frac{1}{V^2} \Omega \right) \boldsymbol{\xi} - \mathbf{C}_{\mathcal{Q}}(\boldsymbol{\xi}, \bar{\omega}) = \mathbf{0}. \quad (1)$$

For the present analysis, we consider a linear structural model expressed in terms of structural natural modes together with a nonlinear aerodynamic model. Structural damping is neglected. k_w is a constant de-

pendent on the wing shape and overall mass given by

$$k_w = \frac{\pi A_{\mathbf{R}} (1 + \lambda_t) (1 + \lambda_t + \lambda_t^2)}{6 \bar{m}}, \quad (2)$$

and $\mathbf{C}_{\mathcal{Q}}$ is the vector of generalized aerodynamic forces, the m^{th} element of which is given by

$$C_{\mathcal{Q}m} = \frac{1}{q_{\infty} c_r^2} \iint_A \bar{p}_1 \psi_m \cdot \hat{\mathbf{n}} \, dA \quad (3)$$

where the integral is evaluated over the surface of the wing.

One can also include the static (i.e. mean flow) aeroelastic equations in the mathematical model. However for the case of the AGARD 445.6 wing configuration, this is not necessary since the configuration consists of a wing based on a constant symmetric airfoil section at a mean angle-of-attack of zero degrees. As such, no net steady, or static, aerodynamic load acts on the wing.

In order to solve the aeroelastic system (Eq. 1), one must be able to compute the generalized aerodynamic forces $\mathbf{C}_{\mathcal{Q}}$ for finite values of the structural modal coordinates $\boldsymbol{\xi}$. This is the role of the harmonic balance solver. Details of the harmonic balance procedure can be found in Refs. [1-4].

Limit Cycle Oscillation Solution Procedure

Based on previous research efforts conducted for two-dimensional airfoil configurations (Ref. [2,3]), and three-dimensional inviscid flow wing configurations (Ref. [4]), we have found that a Newton-Raphson technique in conjunction with the harmonic balance nonlinear unsteady flow solver technique provides an efficient method for determining limit cycle oscillation response.

As has been demonstrated in Thomas et. al.,²⁻⁴ the harmonic balance LCO solution method proceeds by choosing one of the structural modal coordinates to be the independent variable. For three-dimensional flow about wings, we consider ξ_1 , the modal coordinate of the first (typically first bending) structural mode shape, as the independent variable. We also chose ξ_1 to be real valued.

In formulating the HB/LCO solution technique, one then proceeds by dividing Eq. 1 through by ξ_1 , and re-expressing the system of equations as:

$$\begin{aligned} \mathbf{R}(\mathbf{L}, \xi_1) &= k_w \mathcal{M} \left(-\bar{\omega}^2 \mu \mathbf{I} + \frac{1}{V^2} \Omega \right) \frac{\boldsymbol{\xi}}{\xi_1} - \mathbf{C}_{\mathcal{Q}} \left(\frac{\boldsymbol{\xi}}{\xi_1}, \xi_1, \bar{\omega} \right) \\ &= \mathbf{0}. \end{aligned} \quad (4)$$

Considering both the real and imaginary parts of Eq. 4, the vector \mathbf{L} then represents the unknown LCO

solution variables

$$\mathbf{L} = \left\{ \begin{array}{c} V \\ \bar{\omega} \\ \text{Re}(\xi_2)/\xi_1 \\ \text{Im}(\xi_2)/\xi_1 \\ \vdots \\ \text{Re}(\xi_M)/\xi_1 \\ \text{Im}(\xi_M)/\xi_1 \end{array} \right\}, \quad (5)$$

which consists of the LCO reduced velocity V (this variable is customarily the independent variable in time-domain LCO solution techniques), LCO reduced frequency $\bar{\omega}$, and the real and imaginary parts of the ratio of each of the LCO structural modal coordinates, for modes two and higher, to the first structural modal coordinate amplitude ξ_1 . The real and imaginary parts of Eq. 4 as such represent a system of $2M$ equations for the $2M$ unknown LCO solution variables of \mathbf{L} .

As observed in Thomas et. al.,²⁻⁴ an efficient method for solving Eq. 4 is to use a simple Newton-Raphson root finding technique. This is an iterative method for solving for the unknown LCO variables \mathbf{L} whereby one “marches” the vector equation

$$\mathbf{L}^{n+1} = \mathbf{L}^n - \left[\frac{\partial \mathbf{R}(\mathbf{L}^n)}{\partial \mathbf{L}} \right]^{-1} \mathbf{R}(\mathbf{L}^n), \quad (6)$$

until a suitable level of convergence is achieved.

We have also observed that one can use simple forward finite-differencing to compute the column vectors of $\partial \mathbf{R}(\mathbf{L})/\partial \mathbf{L}$. That is,

$$\left[\frac{\partial \mathbf{R}(\mathbf{L})}{\partial \mathbf{L}} \right] = \left[\begin{array}{c|c|c|c} \frac{\partial \mathbf{R}}{\partial V} & \frac{\partial \mathbf{R}}{\partial \bar{\omega}} & \frac{\partial \mathbf{R}}{\partial \text{Re}(\xi_2)/\xi_1} & \frac{\partial \mathbf{R}}{\partial \text{Im}(\xi_2)/\xi_1} \\ \hline & & & \\ \hline & & & \\ \hline & & & \end{array} \right], \text{ etc.} \quad (7)$$

where for example

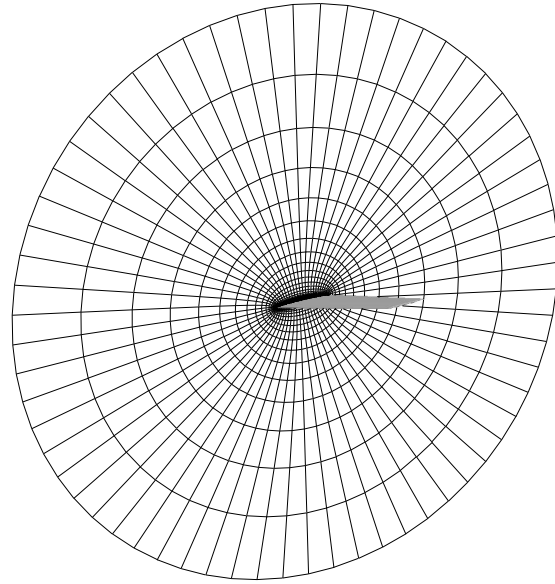
$$\frac{\partial \mathbf{R}(\mathbf{L})}{\partial V} \approx \frac{\mathbf{R}(\mathbf{L}, V + \epsilon) - \mathbf{R}(\mathbf{L}, V)}{\epsilon},$$

$$\frac{\partial \mathbf{R}(\mathbf{L})}{\partial \bar{\omega}} \approx \frac{\mathbf{R}(\mathbf{L}, \bar{\omega} + \epsilon) - \mathbf{R}(\mathbf{L}, \bar{\omega})}{\epsilon},$$

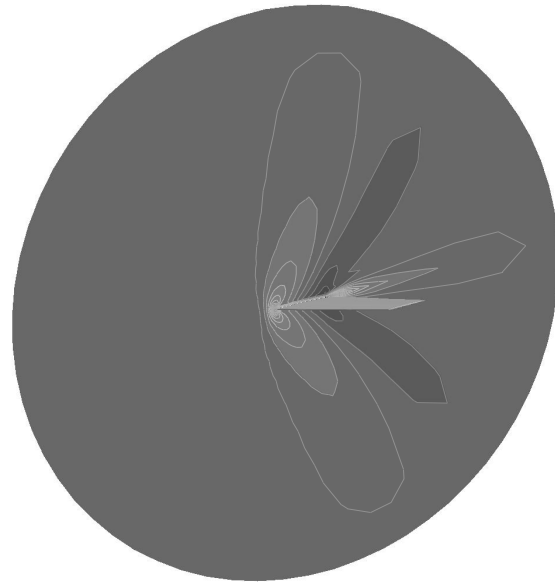
etc. for a small ϵ . Determining the column vectors of $\partial \mathbf{R}/\partial \mathbf{L}$ in this manner thus requires numerous computations of $\mathbf{R}(\mathbf{L})$ for various perturbations to \mathbf{L} . This in turn means several computations of the unsteady aerodynamic loading \mathbf{C}_Q for the different perturbations of \mathbf{L} , and this is where the harmonic balance solver is utilized.

The AGARD 445.6 Transonic Wing

As noted in the introduction, the AGARD 445.6 transonic wing aeroelastic configuration^{5,6} is considered. This is a 45 degree quarter chord swept wing



a) Computational Grid



b) Mach Contours

Fig. 2 AGARD 445.6 Wing Viscous Case Wing Viscous Grid Topology and Mach Contours for $M_\infty = 1.141$

based on a NACA 65A004 airfoil section, which has an aspect ratio of 3.3 (for the full span), and a taper ratio of 2/3.

Figure 2a illustrates the viscous computational mesh used in the current analysis for this configuration, and Fig. 2b shows computed Mach number contours for $M_\infty = 1.141$, and $Re_\infty = 860,000$. The grid is based on an “O-O” topology, slightly different than that of Ref. [4], which better resolves flow in the wing tip region. The mesh uses 65 (mesh i coordinate) computational nodes about the wing in the stream-

wise direction, 33 (mesh j coordinate) nodes normal to the wing, 13 (mesh k coordinate) nodes along the semi-span, and 12 more nodes wrapping around the wing tip. The total number of fluid dynamic degrees-of-freedom for this CFD mesh is thus $321,750$ (i.e. dependent flow variables $(6) \times i_{max}(65) \times j_{max}(33) \times k_{max}(33)$). The outer boundary of the grid extends five wing semi-spans from the mid-chord of the wing at the symmetry plane. The particular structural configuration of the wing under consideration is referred to as the “2.5 ft. weakened model 3”^{5,6}. For the results presented in this study, the CFD method is a variant of standard Lax-Wendroff scheme^{10,11} in conjunction with the one-equation turbulence model of Spalart and Allmaras.¹²

Nonlinear Unsteady Aerodynamics

To demonstrate nonlinear unsteady aerodynamic effects brought about by finite amplitude motions, we compute the unsteady aerodynamic response for a $M_\infty=1.141$ background steady flow condition about the AGARD 445.6 wing configuration for various finite amplitudes of unsteady wing motion. We choose a reduced frequency of $\bar{\omega} = 0.1$ since this is near the reduced frequency at which the wing flutters, and we consider the first torsional modal coordinate ξ_2 in this instance.

Figure 3a and Fig. 3b show computed real and imaginary parts, respectively, of the second modal generalized force coefficient C_{Q_2} normalized by the second modal coordinate ξ_2 as a function of the magnitude of second modal coordinate. Two harmonics are used in the harmonic balance method.

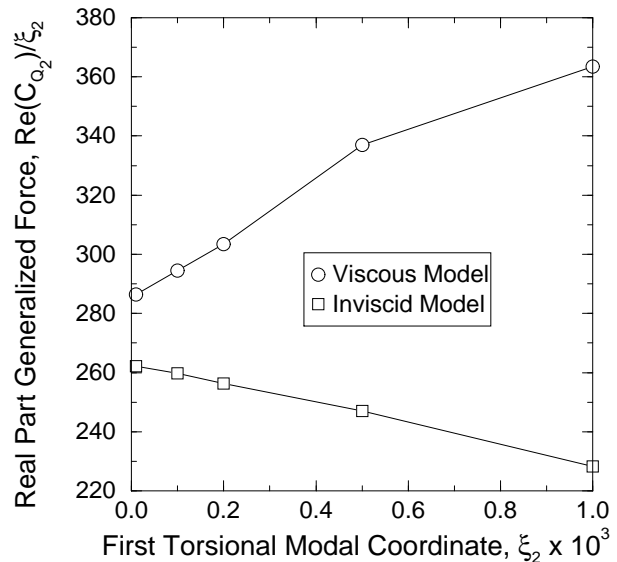
To give the reader a sense of the physical displacement of the wing associated with the magnitude of second modal coordinate ξ_2 , a value of $\xi_2 = 0.001$ corresponds to a maximum vertical, normal to the wing surface, unsteady displacement of the wing approximately two percent relative to the semi-span of the wing.

As can be seen from Fig. 3, nonlinear effects due to finite amplitude motion are readily apparent for both the viscous and inviscid flow models. Even more so for the viscous case.

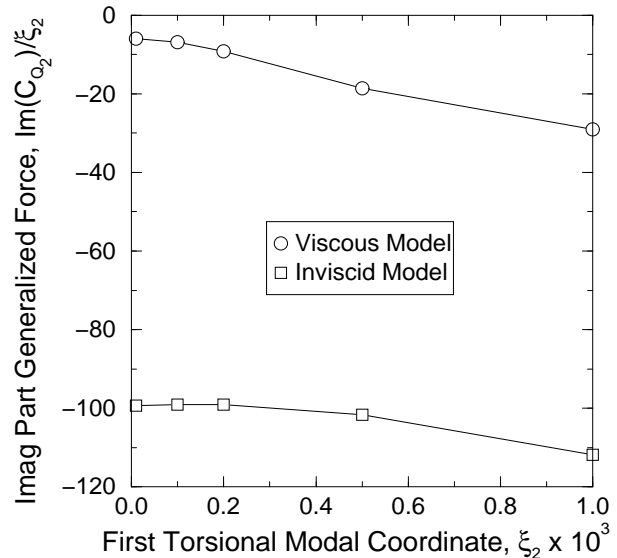
Nonlinear Aeroelasticity and LCO

Table 1 shows computed values for the LCO reduced velocity V , reduced frequency $\bar{\omega}$, and the shape of the unsteady motion of the wing near the flutter onset condition. That is, for a very small value of first structural mode shape modal coordinate. In this case, $\xi_1 = 0.00001$. As ξ_1 goes to zero, we eventually recover the linear small disturbance flutter onset condition.

The structural data is presented in terms of the ratio of the amplitude of each of the structural modal coordinates normalized to the amplitude of first structural modal coordinate. As can be seen, the first bending



a) Real Part



b) Imaginary Part

Fig. 3 Unsteady Generalized Force as a Function of Mode Shape Amplitude for Wing First Torsional Mode.

structural motion dominates near the flutter onset condition for the inviscid case. However for the viscous flow model, it is interesting to note that the second mode, in this case the first torsional mode shape, is much more significant near the flutter onset condition. The first four structural modes have been considered in the analysis. The significant reduction in the value for the reduced velocity is consistent the trends observed with the computational studies of Lee-Rausch et. al.^{7,8} and Gordnier and Melville.⁹ In this present study, we again note that have used a different grid topology

	Inviscid	Viscous
V	0.597	0.500
$\bar{\omega}$	0.0860	0.142
$\text{Re}(\xi_2)/\xi_1$	-0.207	-1.02
$\text{Im}(\xi_2)/\xi_1$	0.0146	0.145
$\text{Re}(\xi_3)/\xi_1$	0.0804	0.277
$\text{Im}(\xi_3)/\xi_1$	-0.00665	-0.0104
$\text{Re}(\xi_4)/\xi_1$	0.0223	0.0332
$\text{Im}(\xi_4)/\xi_1$	-0.00258	-0.0125

Table 1 AGARD 445.6 Wing Configuration Mach Number Near the Flutter Onset Conditions. $\xi_1 = 0.00001$, $M_\infty = 1.141$, and $Re_\infty = 860,000$ for Viscous Case.

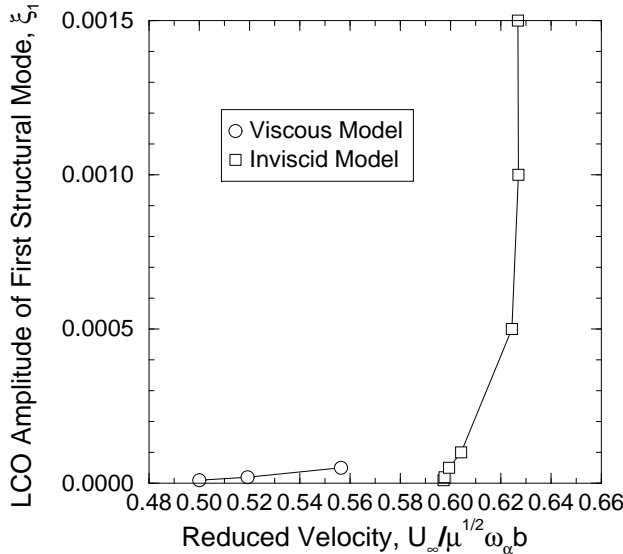


Fig. 4 Computed AGARD 445.6 Wing Configuration LCO Characteristics. $M_\infty = 1.141$, and $Re_\infty = 860,000$ for Viscous Case.

from that of Ref. [4]. As such, we have found that we obtain a slightly different reduced velocity value near the flutter onset condition from that of Ref. [4] for the inviscid case. Finally, Fig. 4 shows sample computed LCO solutions for the viscous and inviscid flow models of the 445.6 wing configuration for the $M_\infty = 1.141$ flow condition. Shown is the LCO amplitude of the first structural modal coordinate, ξ_1 , versus the reduced velocity V . The beginnings of a stable nonlinear LCO behavior trend is apparent for the viscous flow model for very small amplitudes of motion. Additional viscous LCO computations are currently underway for larger amplitudes. Linear aeroelastic LCO behavior for the inviscid flow model is apparent for larger amplitudes of motion.

Conclusions

A harmonic balance method for modeling nonlinear periodic unsteady three-dimensional inviscid and viscous transonic flows about wing configurations is

presented. Demonstrated is the ability of the method to model nonlinear aerodynamic effects due to finite amplitude motions for the well known AGARD 445.6 aeroelastic configuration at a supersonic flow condition. A limit cycle oscillation solution methodology is also presented and demonstrated for the same benchmark transonic configuration. The beginnings of a stable LCO trend is observed for the viscous flow case for very small amplitude motions. Further computational studies are currently underway.

Acknowledgments

This work was supported by AFOSR grant, "Limit Cycle Oscillations and Nonlinear Aeroelastic Wing Response: Reduced Order Aerodynamics" and STTR grant, "Nonlinear Reduced Order Modeling of Limit Cycle Oscillations of Aircraft Wings/Stores". The latter grant is joint work with Zona Technology. Dean Mook is the AFOSR Program Manager.

References

- ¹Hall, K. C., Thomas, J. P., Clark, W. S., "Computation of Unsteady Nonlinear Flows in Cascades Using a Harmonic Balance Technique", *AIAA Journal*, Vol. 40, No. 5, 2002, pp. 879-886.
- ²Thomas, J. P., Dowell, E. H., Hall, K. C., "Nonlinear Inviscid Aerodynamic Effects on Transonic Divergence, Flutter and Limit Cycle Oscillations", *AIAA Journal*, Vol. 40, No. 4, 2002, pp. 638-646.
- ³Thomas, J. P., Dowell, E. H., Hall, K. C., "Modeling Viscous Transonic Limit Cycle Oscillation Behavior Using a Harmonic Balance Approach", AIAA Paper 2002-1414, 43th AIAA/ASME/ASCE/AHS/ASC Structures, Structural Dynamics and Materials (SDM) Conference, Denver, CO, April 2002.
- ⁴Thomas, J. P., Dowell, E. H., Hall, K. C., "A Harmonic Balance Approach for Modeling Three-Dimensional Nonlinear Unsteady Aerodynamics and Aeroelasticity", ASME Paper IMECE-2002-32532, Proceedings of the ASME International Mechanical Engineering Conference and Exposition, November 17-22, 2002, New Orleans, Louisiana, USA.
- ⁵Yates, E. C., Jr., "AGARD Standard Aeroelastic Configurations for Dynamic Response I - Wing 445.6", NASA TM 100492, August 1987; also *Proceedings of the 61st Meeting of the Structures and Materials Panel*, Germany, AGARD-R-765, 1985, pp. 1-73.
- ⁶Yates, E. C., Jr., Land, N. S., and Foughner, J. T., Jr., "Measured and Calculated Subsonic and Transonic Flutter Characteristics of a 45 Deg Sweptback Wing Planform in Air and in Freon-12 in the Langley Transonic Dynamics Tunnel", NASA TN D-1616, March 1963.
- ⁷Lee-Rausch, E. M. and Batina, J. T., "Wing Flutter Boundary Prediction Using Unsteady Euler Aerodynamic Method", *Journal of Aircraft*, Vol. 32, No. 2, 1995, pp. 416-422.
- ⁸Lee-Rausch, E. M. and Batina, J. T., "Wing Flutter Computations Using an Aerodynamic Model Based on the Navier-Stokes Equations", *Journal of Aircraft*, Vol. 33, No. 6, 1995, pp. 1139-1147.

⁹Gordnier, R. E., Melville, R. B., “Transonic Flutter Simulations Using an Implicit Aeroelastic Solver”, *Journal of Aircraft*, Vol. 37, No. 5, 2000, pp. 872–879.

¹⁰Ni, R., “A Multiple Grid Scheme for Solving the Euler Equations”, *AIAA Journal*, Vol. 20., pp. 1565–1571, November, 1982.

¹¹Saxor, A. P., “A Numerical Analysis of 3-D Inviscid Stator/Rotor Interactions Using Non-Reflecting Boundary Conditions”, Gas Turbine Laboratory Report 209, MIT March 1992.

¹²Spalart, P. R., and Allmaras, S. R., “A One Equation Turbulence Model for Aerodynamic Flows”, AIAA Paper 92-0439, January, 1992.